

Particle-Transfer Between the Cyclone and Accumulator Sections of a Desander

C. H. Rawlins, eProcess Technologies

Summary

The flooded-core solid/liquid hydrocyclone, also called a desander, is often used in the upstream oil and gas industry to separate particulate solids from produced water. A desander incorporates a solid/liquid cyclone with an accumulation chamber connected to the apex. Solids collect in the accumulator for intermittent removal while the overflow is discharged continuously. With a flooded-core and static-liquid volume in the accumulator, the trajectory of a sand particle from the cyclone inlet to the apex is changed, compared with that in an open underflow hydrocyclone classifier. In this project, the transfer of solids from the cyclone to the accumulator section is studied, with emphasis on the limiting flux. The settling of solids from the cyclone to the accumulator follows a turbulent, hindered-settling relationship that can be approximated by models used for sedimentation hoppers. Measurement of the apex-flux rate shows a maximum choke point, beyond which solids will back up into the cyclone section. The limiting inlet solids concentration to reach this choke point is ≈ 2 g/L for small-diameter desanders. An apex-flux balancing system is proposed to overcome this flux-rate limitation.

Introduction

Sand and/or solids are often present in the produced-water streams of oil and gas production systems (Hodson et al. 1994; Lohne 1994; Rawlins 2013a). Sand reports to the processing facilities from oil and gas production wells. Large sand particles (>200 μm) settle in the low-velocity zones of the production separator and free-water knockout (FWKO) vessels. Commonly, sand that fills these vessels is removed by jetting or manual-cleaning operations. Intermediate-sized sand, typically 25 to 200 μm in diameter, flows with the water phase to exit the production separators (Rawlins 2013b). Small solids, typically <25 μm , stay in the oil phase or collect at the oil/water interface. The intermediate-sized solids that discharge with the water phase erode control valves and any deoiling hydrocyclones, fill flotation cells, plug media and cartridge filters, increase the oil-in-water values (because of oil coating), and may obstruct water-injection reservoirs (Lohne 1994). Desanding hydrocyclones, shown in Fig. 1, are used commonly to remove intermediate solids from produced water to protect produced-water-treatment systems.

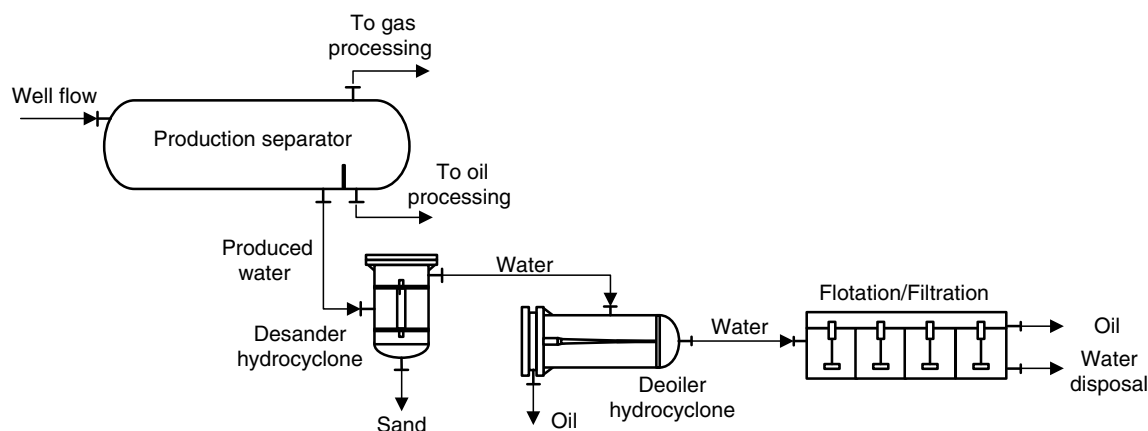


Fig. 1—Process-flow schematic of a possible well fluid-processing system with emphasis on produced-water treatment. A desander hydrocyclone is the first stage of produced-water treatment, and is used to remove sand and to protect downstream oil-removal equipment.

Desanding hydrocyclones, also called desanders, are directly on the water outlet of a three-phase separator or FWKO. They should be upstream of deoiling hydrocyclones and the liquid-level control valve (Ditria and Hoyack 1994; Lohne 1994). The produced water exiting the separator generally has a <0.1 g/L (100 ppmw) sand concentration, with a particle size ranging from 25 to 200 μm , with 125 μm as the mean. Desanders operate by using the inherent pressure from the upstream vessel, and require 0.34- to 3.45-bar differential pressure to operate. They are a static device with no moving parts and have replaceable wear components. A desander used as the first stage of treatment of the produced-water stream will protect downstream components and does not degrade subsequent removal of oil from the produced water.

Desander Operability. Cyclonic technology, within which desanders fall as a unit process, requires a pressure differential and geometric shape of the device to create a swirling flow pattern that allows phase separation. Cyclonic technology has the highest throughput-to-size ratio of any separation method (Rawlins and Wang 2000). Where this technology can be applied, for a given flow rate, it will have the smallest footprint and weight of any separation technology, which is an advantage in offshore and subsea systems. In addition,

cyclonic devices are unaffected by facility motion (necessary on floating systems) or orientation. The vortex flow generates between 100 and 5,000 times the acceleration caused by gravity (g -forces), depending on the diameter and pressure drop.

Desanders are designed specifically for particulate-solids removal from a fluid stream. Two styles of desanders have found use in the upstream petroleum industry. Fig. 2 shows the single-cone (insert) vs. the multicone (liner) design. Both designs are made from a pressure-vessel housing containing one or more cyclonic inserts or liners. The insert style has a single cyclone, whereas the multicone style has multiple cyclones operating in parallel. The insert and liner are each replaceable within the vessel, and are designed to create the cyclonic flow pattern and contain any erosive flow, whereas the pressure vessel contains the operating pressure and does not encounter any wear. Both styles have an inlet connection, a clean-water fluids outlet, and an integral accumulation chamber (accumulator) for the collection and periodic discharge of the separated solids.

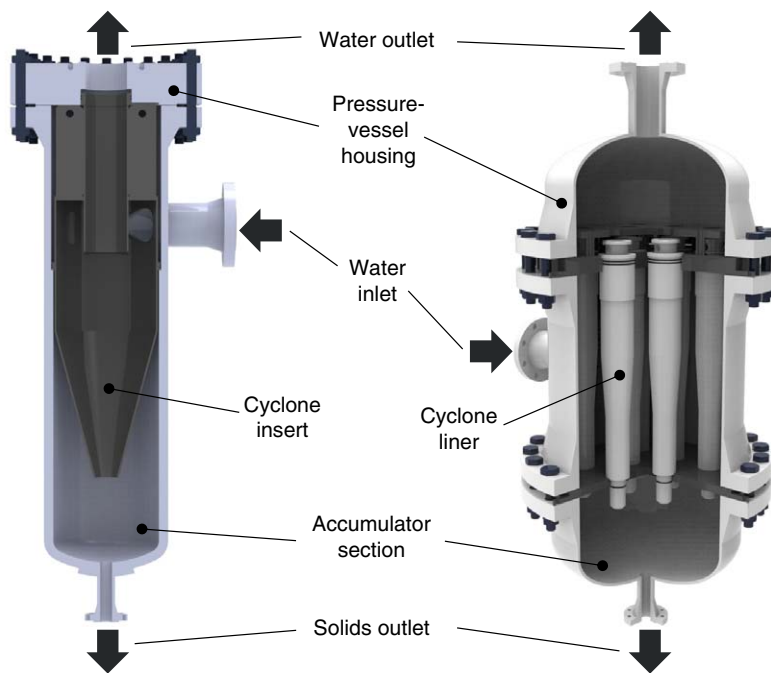


Fig. 2—Cross-section schematics of two styles of desanding vessels: insert style (left) and liner style (right).

The primary operating difference between the insert and liner styles is the handling of incoming fluids. In the single-cone design, all fluids are contained within the one cyclonic insert. However, incoming fluids in the multicone style are dispersed within the inlet chamber and then distributed to each individual cyclonic liner. In multiphase flow (e.g., wellhead desander), the multicone style does not distribute the same proportion of gas and liquid flow equally to each liner, and variable performance can be exhibited (e.g., some liners will contain more gas, and some will contain more liquid). The single-cone style treats multiphase fluid in one device without unequal gas/liquid partitioning, thereby providing consistent-separation efficiency. The insert style provides better performance in multiphase desanding.

With cyclonic devices, separation size is proportional to diameter. In treating water, a 38-mm-diameter cyclone has a separation size of 10 μm , whereas 76- and 254-mm cyclones have 30- and 60- μm separation sizes, respectively. Multicone desanders, with many small-diameter cyclones in parallel, are preferred for liquid-only applications in treating the higher-viscosity fluid. Single-cone desanders work well in multiphase-flow scenarios in which the incoming fluid is a mixture of gas and liquid, and the mixture-phase fluid, therefore, has a low viscosity and a low density. A 254-mm insert-desander processing a 95% gas-void-fraction (GVF) fluid can achieve a separation size of less than 15 μm .

Liner-style desanders have a higher solids-removal efficiency in liquid applications; however, they are limited with respect to the particle size that they can handle without plugging. Cyclone liners have a 6- to 12-mm critical orifice diameter (either inlet width or apex diameter), and particles exceeding this size will plug the liners. However, insert-style desanders, with much larger critical orifice diameters, can handle particles up to 25 to 50 mm in diameter. These larger-sized particles are not commonly observed in produced-water streams, but are present in raw well flow. Therefore, single-cone desanders are better for wellhead applications.

Originally, desanders were developed in the 1950s for treating agriculture water to prevent sand particles from plugging irrigation nozzles. Generally, this application involves a low concentration of sand (<0.01 g/L). Because of the simple design and efficient operation of desanders, this technology was transferred to produced-water treatment in the 1960s. However, the concentration of sand experienced was much higher than in agricultural applications. The initial rule-of-thumb design for the maximum inlet solids concentration that a desander could treat was 1 vol% (26.5 g/L). This value worked sufficiently for large-diameter desanders (>762 mm). However, as more-efficient solids capture was sought, the multicone-style desanders became more prevalent, resulting in cyclone diameters decreasing to 76, 51, and 25 mm. The 1 vol% rule of thumb proved to be incorrect for these sizes. The small liners showed both plugging and premature wear failure in many applications. A more accurate maximum concentration value was required, especially a method applicable across a range of operating conditions and cyclone diameters. The present work was undertaken to measure the maximum inlet concentration that small-diameter cyclones can treat without plugging, and to determine a sizing method to apply to the range of desander diameters.

Effect of Solids Concentration on Operation. The solid/liquid hydrocyclone was introduced in the 1890s and finds primary use in the mineral-processing industry. Grinding of ore to liberate valuable minerals involves banks of hydrocyclones (typically 254 to 1016 mm

in diameter) as a classifying device in closed-circuit arrangements. These hydrocyclones are operated at low pressure (inlet < 1.4 barg) with atmospheric underflow and overflow discharge, and they process slurry streams with 20- to 40-wt% solids. The underflow fraction, which contains coarse solids, is returned to the mill inlet for further grinding, whereas the overflow stream contains the fine-solids portion that is sent to downstream processing (typically, for flotation).

A mineral hydrocyclone has an open underflow stream, discharging at atmospheric pressure. The concentrated discharge slurry discharges continuously and collects into an open launder or trough. A desander, by contrast, has a fully enclosed underflow stream in which the solids are collected into an accumulator chamber that fully encapsulates the underflow orifice (apex). The solids are then discharged intermittently (batch) from the system. The solids in a desander are concentrated as they spin down the length of the cone and exit the apex into the accumulation chamber. The accumulation chamber contains a constant volume of water, and the solids exiting the apex displace the accumulator water, which then returns through the apex back into the cyclone body. The accumulator water is discharged eventually through the overflow. This effect is illustrated in the circled area of Fig. 3.

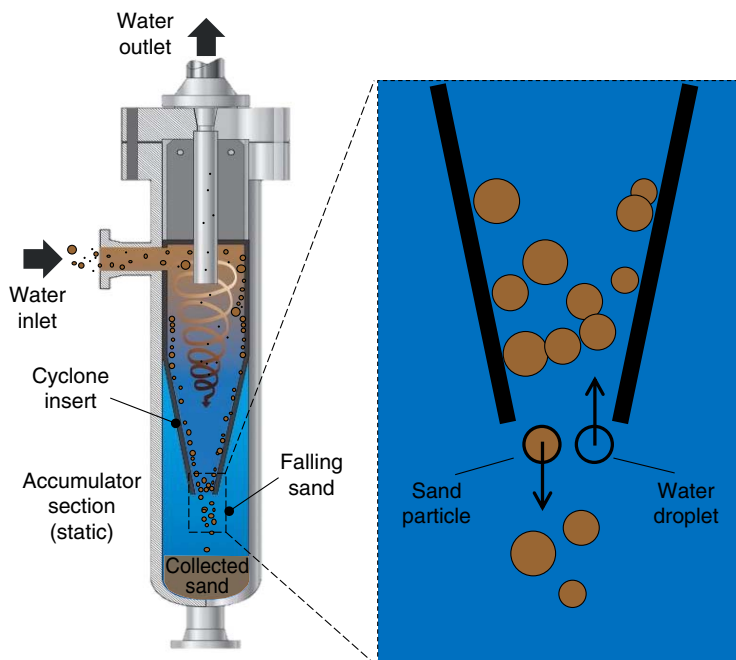


Fig. 3—Schematic of a single-cone desander, showing the solid/fluid volume swapping that occurs as particles discharge through the apex and enter the accumulation chamber. The accumulator contains a static liquid at a fixed volume (the valve that closes the bottom outlet is not shown).

The volume of solids flowing downward, entering the accumulation chamber, displaces an equal volume of water flowing upward through the apex, which has been termed “volume swapping” (Rawlins 2002). Volume swapping occurs because of the density differential between the solids and water. As the particle “falls” into the accumulator, the downward trajectory of the particle is opposed slightly by the upward flow of the water, which reduces the net terminal velocity. At low solids concentrations, the terminal-velocity reduction is negligible; however, as the concentration of solids discharging the apex increases, the amount of liquid returning will eventually choke the downward solids flow. Therefore, a maximum flux exists at which the desander can operate. Above this flux limit, solids will collect at the apex entrance and back up into the cone section. This effect is illustrated in Fig. 4. As the solids level rises in the cone section, the cyclonic body (cylinder and cone sections) fills; the solids eventually will report to the vortex finder (thus, degrading separation efficiency). Laboratory investigations have shown that the cyclonic body in a 51-mm-diameter desander can be filled within a few minutes at a high solids concentration.

Another effect of aggregated solids collecting above a choked apex is premature erosive failure in the cone section of the liner. With a choked apex, a high-velocity spinning fluidized bed of solids exists above this point. This concentrated solid-bed erodes the liner cone, as shown in Fig. 5. The 38-mm-diameter desander liner in this photo experienced premature failure in the cone section because of the choking of the apex. The desander was installed for treating produced water with 0.25 g/L of solids; however, the operator used the desander to treat a separator jetting stream with up to 100 g/L of solids. The high concentration of solids overwhelmed the desander, and solids were trapped in the cone section, unable to report to the accumulator. These spinning solids eroded the cone section until the cone wall was breached.

Studies on Flooded-Core Hydrocyclones. Operating a hydrocyclone with open underflow results in a central air core that exists throughout the full length of the cyclonic body (from the apex to the vortex finder) and has a slight negative pressure (Svarovsky 1984). Converting a hydrocyclone to a desander by encapsulating the apex orifice floods the cyclone internally and prevents the formation of an air core. Thus, a desander can be termed a “flooded-core hydrocyclone.” The body of scientific literature on hydrocyclone operation and modeling pertains to open-underflow designs containing an air core (Plitt 1976). A few studies have been conducted with flooded-core, solid/liquid hydrocyclones; however, no studies were conducted with a static-accumulation chamber. Researchers at McMaster University studied the velocity distribution in a 76-mm glass hydrocyclone, operating without an air core (Knowles et al. 1973). They connected the underflow to a pipe network that encapsulated the apex; however, the system was operated by continuously pulling fluid away from the underflow, thus preventing a static-fluid chamber. The operating conditions were set so that the underflow and overflow streams had similar flow rates. Only velocity profiles were measured with tracer particles and high-speed photography. The tangential, vertical, and radial profiles were found to resemble an open-underflow hydrocyclone. Further research was conducted with the same

setup, in which the researchers varied the underflow/overflow split and measured the classification performance (Witbeck and Woods 1984). Their results showed a less-sharp (flatter) classification curve with the flooded hydrocyclone and a pressure drop 4–7 times greater than that in an open-underflow system (note that the current body of work showed a negligible difference in pressure drop when comparing open and flooded underflows). Researchers at Northeast University of Technology (Shenyang, China) measured the performance of 51- and 76-mm water-sealed hydrocyclones (Quian et al. 1989). Resembling the work at McMaster University, they withdrew a liquid stream from the underflow chamber, which negated the formation of a static bed of water. When comparing the performance of the hydrocyclone with flooded underflow with that of the open-underflow configuration, they measured a slightly greater solids recovery and a 1.6-fold increase in pressure drop in the flooded-underflow case. When enclosing the underflow stream, they increased the apex diameter by 10 times to minimize blockage potential. In these studies, the investigators removed the air core by encapsulating the underflow stream; however, they negated the development of a static-fluid chamber by withdrawing fluid continuously from the accumulation chamber.

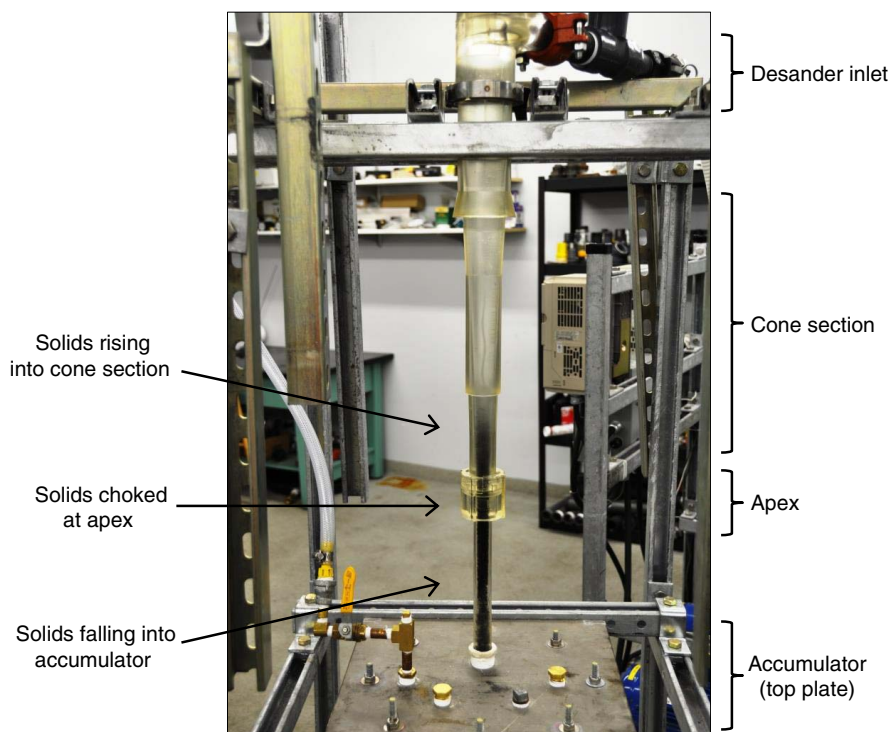


Fig. 4—A 51-mm-diameter clear hydrocyclone, configured as a desander connected to a large-diameter accumulator chamber. The desander is operating at a 1.4-bar pressure drop, and is processing 12/20-mesh coal particles (used to show the particle-flow pattern). The particles have exceeded the apex-flux limit and are collected in the lower-cone section. Eventually, the level of solids will rise to the vortex finder, resulting in degraded separation performance.

Laboratory Testing

The main goal of this research project was to determine the maximum solids-flux rate, as a function of inlet-stream solids concentration, that could pass through the desander apex into a static liquid-accumulation chamber. **Fig. 6** shows a photograph of the test loop built for this study, which consisted of a feed-mixture tank, centrifugal pump with piping and instruments, and a 51-mm-diameter hydrocyclone that could be operated with open or enclosed underflow.

The inlet mixture of sand and water was prepared in a 227-L cone-bottom tank. Particulate solids were added into the tank by means of a vibratory feeder, and the sand was distributed by using a pneumatic mixer. Inlet concentrations accurate to 0.1 g/L could be prepared. The feed stream was delivered at the desired flow rate by a centrifugal pump controlled with a variable-frequency drive. The inlet pressure to the test hydrocyclone/desander was measured with a pressure gauge (0.0–2.1 barg). Overflow from the hydrocyclone/desander was returned at atmospheric pressure to the mixing tank, making a closed-circuit test loop. The test desander consisted of a 51-mm-diameter clear urethane (commercial) hydrocyclone connected to a 51-mm-diameter clear cylindrical accumulation chamber (610 mm long with 10-cm³ gradation marks). The hydrocyclone dimensions included a 161-mm² inlet area, a 19.1-mm-diameter vortex finder, and a 15.9-mm-diameter apex.

A test slurry was made with municipal water (1007-kg/m³ density and viscosity of 1.014×10⁻³ Pa·s at 15°C) mixed with test sand. Two test sands were used, each composed of crystalline silica (SiO₂) with a density of 2660 kg/m³. The coarse test sand had a particle size ranging from 38 to 600 μm in diameter. The < 38-μm fraction of this sand was removed by wet sieving. The fine test sand had a measured median particle size (50% on size distribution, P₅₀) of 12 μm, with 95% passing 45 μm. The coarse and fine sands had a packing void fraction of 47.3 and 44.4%, respectively. Measurements of the sand density, void fraction, and water viscosity were conducted by immersion pycnometry, volumetric analysis, and capillary viscometry, respectively.

An initial hypothetical model was developed that was based on the following premises:

- All solids entering the hydrocyclone report to the apex (i.e., the solids used in testing were large enough to represent 100% recovery). This premise was necessary to form a simple mass balance that was based on the inlet concentration measured without subtraction of particles reporting to the overflow.
- Particles entering the hydrocyclone travel in a standard vortex pattern from the inlet to the apex.
- After reaching the apex, the rotational motion of the particle is arrested because the liquid in the accumulator is static.
- As an initial estimate, and assuming free settling, the terminal settling velocity (u_t) for particles falling through the apex into the static liquid in the accumulator was approximated by Stokes' law, shown in Eq. 1. On the basis of this relationship, the apex

threshold concentration is a function of particle size (d), solid/fluid-density differential ($\rho_s - \rho_l$), and liquid viscosity (μ). Standard gravitational acceleration (g) is used because the particle motion is fully arrested, and no cyclonic forces are applied:

$$u_t = \frac{gd^2(\rho_s - \rho_l)}{18\mu} \dots \dots \dots (1)$$

- For every volume of particles that enters the accumulator, an equivalent volume of liquid returns upward through the apex to eventually exit through the hydrocyclone overflow stream.
- The apex represents a choke point in the downward flow of particles from the hydrocyclone to the accumulator. As such, after the choke value (termed “apex threshold”) is reached, the rate at which the particles fall from the choked apex should remain constant. A further increase in inlet concentration would result in deterioration of the hydrocyclone-separation efficiency, as defined by mass balance, because the particles that cannot be pushed through the choked apex will report to the overflow stream.
- Under these premises, we constructed a mechanistic model to provide a first-order estimate of the target concentration.



Fig. 5—Erosion marks on a 38-mm-diameter desander, showing premature failure in the cone section caused by a concentration-choked apex. The solids trajectory is from top to bottom. The cone section (top) shows severe wear to failure, whereas the apex (bottom) shows negligible erosion.



Fig. 6—Experimental flow-loop setup for testing the desander apex-flux rate. The loop consists of a cone tank with a mixer, variable-drive centrifugal feed pump, and a 51-mm-diameter clear hydrocyclone with a cylindrical accumulator.

The test procedure started with a theoretical inlet concentration that was based on the target particle-size range. A particle-size range was selected for each test with the geometric mean (GM) used as the indicative size (e.g., 106- to 212- μm range; GM = 150 μm). This value was used to set the vibratory-feeder rate (g/min), which would provide the desired inlet concentration in ppm (parts per million by weight). Flow was established through the loop such that the desander exhibited a 1.38-bar pressure drop (5.0- m^3/h flow rate). The desander operating range is 0.34- to 3.45-bar pressure drop, and this operating point was selected as a common design point to balance turndown with pressure consumption. The vibratory feeder and tank mixer were started along with the test time. The slurry was mixed in the tank and allowed to reach a steady state through the loop. Solids fed through the hydrocyclone inlet and traveled in a vortex pattern to the apex. Visual confirmation was used to confirm steady-state particle travel, as shown in Fig. 7.

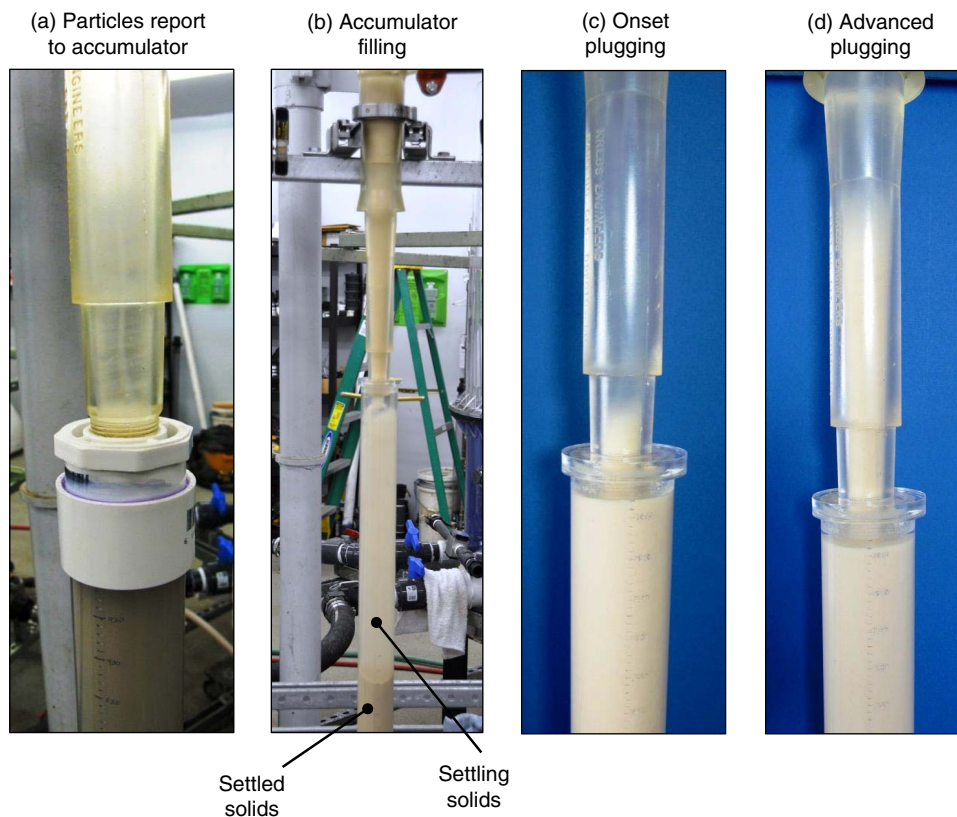


Fig. 7—Photographs showing (a) particles traveling through a hydrocyclone cone section, (b) particles settling and already settled in the accumulator, (c) the onset of apex plugging, and (d) advanced plugging, where solids begin to fill the hydrocyclone body.

The time to fill two 400- cm^3 volumes of the accumulator was recorded. In addition, a visual assessment of the solids level at the cone/apex interface was recorded. If the hydrocyclone appeared to be filling at 7 minutes (Fig. 7d), the test was run for at least 3 more minutes and then stopped. The inlet concentration for that run was deemed to be above the apex threshold. If the cone section was not filled by 10 minutes, the test was stopped, and the inlet concentration was deemed to be below the threshold. If the test conditions were below the apex threshold, the concentration was increased (0.1-g/L increments) for the next run or vice versa if the conditions were above the apex threshold. At the end of each test, the collected solids were dried and weighed. An iterative approach was used until the apex threshold was bracketed by 0.1-g/L concentration. For example, at 150- μm mean particle size, a 2.6-g/L inlet concentration was below the apex threshold, whereas a 2.7-g/L inlet concentration was above the apex threshold. Therefore, the apex threshold was set at the average concentration of 2.65 g/L.

Results and Discussion

Settling Rate. The data for apex solids threshold at five particle sizes are shown in Fig. 8. The GM for each particle-size range was plotted on the abscissa. The ordinate axis represents the inlet solids concentration (g/L) required to reach the apex threshold. The actual data curve shows the limiting line of operation below which the desander operates with steady-state transfer of solids from the cyclone through the apex to the accumulator. Above this curve, the cyclone body will fill with solids because of apex choking; in addition, the rate of filling is proportional to the distance operated above this curve.

The initial hypothetical model was based on Stokes' law (Eq. 1), which is valid only for spherical particles settling in the laminar regime. The actual system uses nonspherical particles settling in a turbulent flow. A revised model was developed that was based on the hindered settling of nonspherical rigid particles in the Newton's-law region (Green and Perry 2008). The first part of the model, shown in Eq. 2, covers free-settling of particles in the turbulent regime ($1,000 < \text{Re} < 350,000$) and incorporates the particle sphericity (ψ). The Reynolds number (Re) for settling particles is shown in Eq. 3:

$$u_t = \sqrt{\frac{4gd(\rho_s - \rho_l)}{3(5.31 - 4.88\psi)\rho_l}} \dots \dots \dots (2)$$

$$Re = \frac{\rho_l u_t d}{\mu} \dots \dots \dots (3)$$

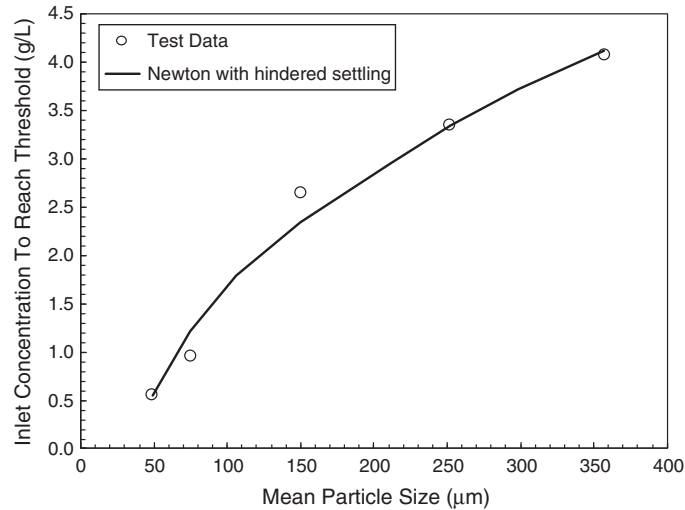


Fig. 8—Comparison of Newton’s-law-based hindered-settling model vs. actual data from apex solids-threshold testing.

Eq. 2 is used for modeling sedimentation hoppers. These hoppers have a fixed volume of liquid into which concentrated sand is introduced and allowed to settle, similar in operation to sand settling in the apex of the cyclone, then to the accumulator (Miedema and Vlasblom 1996). Sand particles introduced into the top of the hopper move downward, and the same volume of water moves upward. In cases of a concentrated mixture with many particles settling in close proximity, a net upward liquid velocity exists that diminishes the particle-settling velocity. This effect is referred to as “hindered settling.” The influence of hindered settling is shown with Eq. 4 (Richardson and Zaki 1954). The corrected settling velocity (u_{th}) is dependent on the volumetric concentration of solids (C_V) and an empirical exponent (m) that can be calculated using Eq. 5:

$$u_{th} = u_t(1 - C_V)^m \dots \dots \dots (4)$$

$$m = \frac{4.7(1 + 0.15Re^{0.687})}{1 + 0.253Re^{0.687}} \dots \dots \dots (5)$$

The calculation of the inlet-solids concentration to reach apex-flux threshold starts with the mean particle size. The number of particles that can fit within the cyclone/apex cross-sectional area is determined from the particle diameter, apex diameter (15.9 mm), and volume concentration (a value of 0.34 was used for all sand sizes). The settling velocity of each particle size is determined from Eqs. 2 through 5. The values used for the equation parameters are $\rho_s = 2660 \text{ kg/m}^3$, $\rho_l = 1004 \text{ kg/m}^3$, $C_V = 0.34$, and $\psi = 0.81$ for coarse sand and $\psi = 0.75$ for fine sand. The number of particles passing per unit time through the apex is determined from the settling rate, which is converted into a mass rate of solids. The inlet concentration (g/L) is then calculated on the basis of this mass rate of solids at the operating liquid-flow rate of 5.0 m³/h. The calculated curve that is based on this approach is shown in Fig. 8. The model fits the test data quite well, and can be used to estimate the inlet concentration to reach the apex threshold within the particle-size range from 49 to 357 μm.

The calculation routine for apex critical flux that is based on inlet-solids concentration can be used to incorporate operating factors experienced by commercial desanders. These factors include varying flow rate, produced-water properties (i.e., differing liquid density and viscosity), and produced-sand properties (i.e., varying density caused by either oil coating or change in base mineral). The starting point is the measurement of the mean particle size, apex diameter, and solids-packing fraction. The settling velocity of each particle size is determined from Eqs. 2 through 5. These equations incorporate variations in liquid density and viscosity, as well as solids density. The number of particles passing per unit time through the apex is determined from the settling rate, which is converted into a mass rate of solids. Then, the inlet concentration (g/L) is calculated on the basis of this mass rate of solids at the operating liquid-flow rate.

Accumulator-Fill Rate. Part of the test procedure involved measuring the rate of solids collection in the accumulator. The collection rate (cm³/s converted to g/s by using the packing void fraction and the solids density) was determined before, during, and after the apex-threshold rate was reached. Fig. 9 shows the results for sand at a 150-μm mean particle size. The x-axis lists the percentage of apex-threshold rate, which previously had been determined for this sand-size range. The y-axis lists the apex-flux rate in g/s. The apex-flux rate increases to a maximum of ≈3.0 g/s at 100% threshold rate, and then slightly decreases to 2.7 g/s above the threshold. These data suggest that solids pass through the apex at all inlet-concentration levels; however, the flux rate through the apex appears to reach a plateau (2.7 g/s, in this case), and, at higher flux, the solids will start to fill the cone section. This estimated maximum apex-flux rate can be used to determine the maximum allowable inlet concentration for operation without filling the cyclone body.

Maximum Flux Rate. The model generated was used to estimate operating curves (mean particle size vs. inlet-threshold concentration) for several larger-diameter desander sizes. These curves are shown on Fig. 10 for desanders with 51- to 254-mm nominal diameters. The same calculation routine for apex critical flux that is based on inlet-solids concentration was followed to make these curves. The calculations started with the mean particle size (x-axis value). The apex diameter was set with a common cyclonic geometry ratio ($D_{apex} \approx 0.3D_{cylinder}$). For example, the apex diameter of a 254-mm-diameter (10 in.) desander is 76 mm (3 in.). The settling velocity of each particle size is determined from Eqs. 2 through 5. The number of particles passing per unit time through the apex is determined

from the settling rate, which is converted into a mass rate of solids. Then, the inlet concentration (g/L) is calculated on the basis of this mass rate of solids at the operating liquid-flow rate.

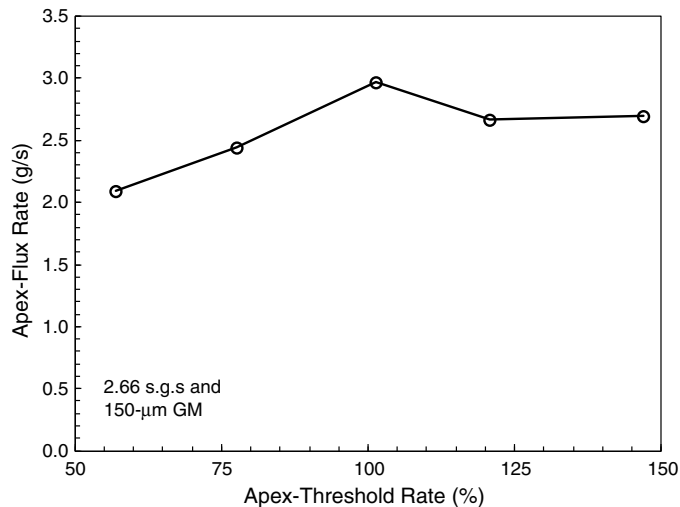


Fig. 9—Apex-flux rate as a function of the percentage of the threshold rate. After reaching a functional threshold, the flux rate seems to settle to a near-constant value.

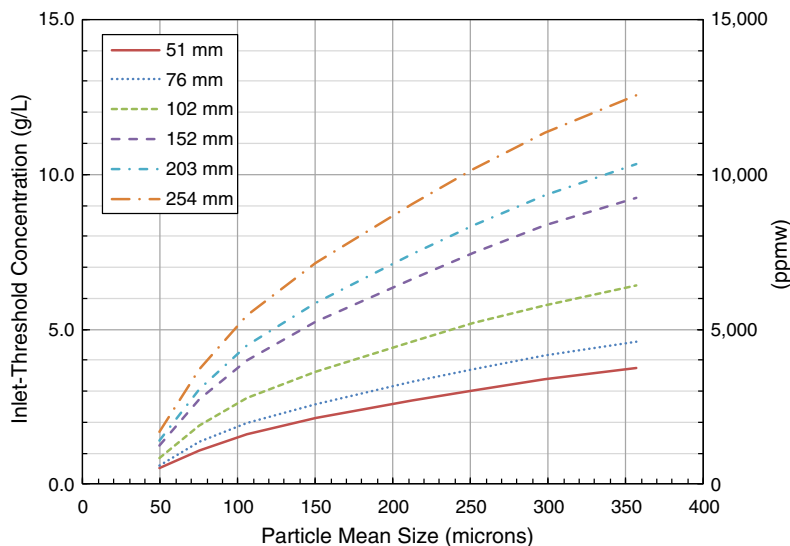


Fig. 10—Calculated curves showing the inlet concentration at which the apex threshold is reached for desanders with various diameters. Values are based on a desander operating at a 1.4-bar pressure drop while treating sand ($\rho_s = 2650 \text{ kg/m}^3$) in fresh water ($\rho_l = 1000 \text{ kg/m}^3$).

To use the curves in Fig. 10, start with the mean particle size on the x -axis, and then look up the operating point for the nominal diameter of the desander in use. For example, a 76-mm desander, separating sand from water with 125- μm mean particle size has a limiting inlet value of $\approx 2.2 \text{ g/L}$ before the apex is choked because of overcrowding. A 204-mm desander has a limiting value of nearly three times that rate ($\approx 6.0 \text{ g/L}$). These curves provide a more accurate guideline than the previously stated 1 vol% rule of thumb. They also show that small-diameter desanders should not be used in high-solids-concentration applications, such as sand-jet slurry or well-flowback operations. In these applications, the solids often exceed 100 g/L .

Recommendation: Apex-Flux Balancing (AFB)

The curves in Fig. 10 show the limiting inlet concentration at which a specific-size desander can operate before the onset of apex choking. These data are modeled for a static-fluid accumulator in which the liquid is displaced upward by the downward-falling particles. Modifying the desander design to allow the liquid in the accumulator to exit the contained volume in a manner other than upward through the apex will increase the allowable flux of particles, thereby enabling the operation of a desander with a much-higher inlet concentration. An apex-flux balance line is installed from the accumulator chamber to an external location at lower pressure. The outward liquid flow is controlled so that the minimum amount is equal to the volume rate of solids entering from the apex. Ideally, the liquid is removed at the same rate as the solids are entering. This method, called AFB, can be used to overcome the threshold induced by a static accumulator. **Fig. 11** illustrates a flow schematic for a single-cone desander with an AFB line installed.

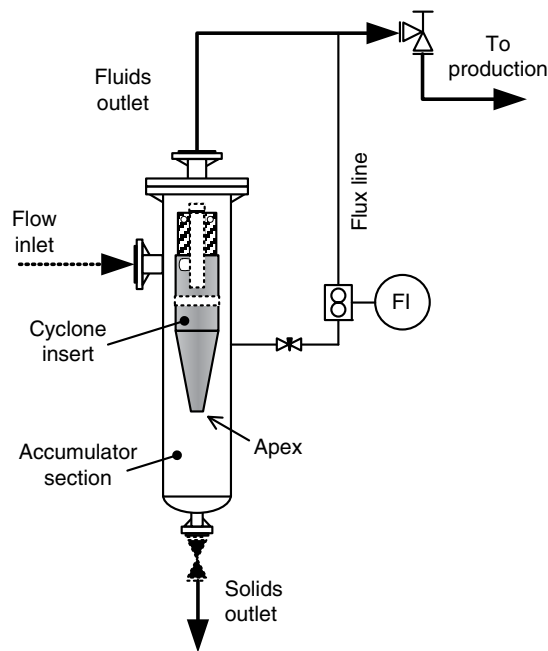


Fig. 11—Flow schematic of single-cone desander with an apex-flux balance line installed. A connection is made to the desander-vessel body, above the apex, to the overflow stream. A valve and flow indicator (FI) are used to balance the liquid-removal rate with the incoming solids-collection rate.

The flux line is connected to the desander-vessel body above the insert apex, which creates a turbulent path, and prevents solids from being pulled into the outflow. The outlet of the balance line is connected to the overflow stream, in this case, which provides a manageable lower-pressure connection point. The flow through this line is controlled with a manual valve and a flowmeter indicator. Ideally, the line, valve, and flowmeter are sized to allow removal of liquid in a controlled manner equal to the volume of solids entering the lower accumulator section. This same configuration can be used with the liner-style desander, with the take-off point connected to the top section of the integral accumulation chamber. In cases of a secondary or external accumulator, the flux line can be attached to the top of this lower vessel; however, it should be designed to minimize solids capture by the fluid-offtake flow.

Conclusions

The desander, a flooded-core solid/liquid hydrocyclone, is a device with a complex fluid-flow pattern. The separation and hydraulic flow-pattern characteristics follow the well-established principles of a hydrocyclone-unit process. The transfer of the separated solids from the cyclonic to the accumulator section (both integral and secondary) follows hindered-settling principles approximated by using Newton's turbulent-settling law. Laboratory analysis of the particle trajectory measured the flux rate of these particles and the effect of solid/liquid volume swapping to yield the apex-threshold value. The apex-threshold value limits the separation efficiency, independent of the cyclone geometric and operational factors. Knowing the characteristics of the inlet solids (particle size and concentration) along with the fluid properties is critical to preventing process inefficiencies that may degrade the separation performance or lead to early mechanical (erosive) failure. The concentration of solids that a desander can treat has a defined value that is based on particle size and fluid properties; for small-diameter desanders (<102 mm) should not be used in high-solids-concentration applications, such as sand jetting or well testing, and cleanup without the operation of an AFB line.

Nomenclature

- C_V = volume concentration (fraction) of solids
- d = particle diameter
- D_{apex} = diameter of the cyclone apex
- D_{cylinder} = diameter of the cyclone cylinder
- g = acceleration caused by gravity
- m = empirical exponent
- P_{50} = measured median particle size (50% on size distribution)
- Re = Reynolds number
- u_t = terminal velocity during free settling
- u_{th} = terminal velocity during hindered settling
- ρ_l = liquid density
- ρ_s = solid density
- μ = liquid viscosity
- ψ = particle sphericity

References

- Ditria, J. C. and Hoyack, M. E. 1994. The Separation of Solids and Liquids With Hydrocyclone-Based Technology for Water Treatment and Crude Processing. Presented at the SPE Asia Pacific Oil & Gas Conference, Melbourne, Australia, 7–10 November. SPE-28815-MS. <https://doi.org/10.2118/28815-MS>.

- Green, D. W. and Perry, R. H. 2008. *Perry's Chemical Engineers' Handbook*, eighth edition. New York: McGraw-Hill.
- Hodson, J. E., Childs, G., and Palmer, A. J. 1994. The Application of Specialist Hydrocyclones for Separation and Clean-Up of Solids in the Oil and Gas Industry. Presented at the 26th Annual Offshore Technology Conference, Houston, 2–5 May. OTC-7590-MS. <https://doi.org/10.4043/7590-MS>
- Knowles, S. R., Woods, D. R., and Feuerstein, I. A. 1973. The Velocity Distribution Within a Hydrocyclone Operating Without an Air Core. *Can. J. Chem. Eng.* **51** (3): 263–271. <https://doi.org/10.1002/cjce.5450510301>.
- Lohne, K. 1994. Separation of Solids From Produced Water Using Hydrocyclone Technology. *Chemical Engineering, Research and Design* **72**: 169–175.
- Miedema, S. A. and Vlasblom, W. J. 1996. Theory for Hopper Sedimentation. Presented at the 29th Annual Texas A&M Dredging Seminar, New Orleans, June.
- Plitt, L. R. 1976. A Mathematical Model of the Hydrocyclone Classifier. *CIM Bull.* **69** (776): 114–123.
- Quian, L., Changlie, D., Jirun, X. et al. 1989. Comparison of the Performance of Water-Sealed and Commercial Hydrocyclones. *Int. J. Min. Proc.* **25** (3–4): 297–310. [https://doi.org/10.1016/0301-7516\(89\)90024-0](https://doi.org/10.1016/0301-7516(89)90024-0).
- Rawlins, C. H. and Wang, I. 2000. Design and Installation of a Sand Separation and Handling System for a Gulf of Mexico Oil Production Facility. Presented at the SPE Annual Technical Conference and Exhibition, Dallas, 1–4 October. SPE-63041-MS. <https://doi.org/10.2118/63041-MS>.
- Rawlins, C. H. 2002. Application of Multiphase Desander Technology to Oil and Gas Production. Paper presented at the BHR 3rd International Conference on Multiphase Technology, Banff, Alberta, Canada, 3–5 June.
- Rawlins, C. H. 2013a. Sand Management Methodologies for Sustained Facilities Operations. Presented at the SPE North Africa Technical Conference and Exhibition, Cairo, 15–17 April. SPE-164645-MS. <https://doi.org/10.2118/164645-MS>.
- Rawlins, C. H. 2013b. Design of a Cyclonic Solids Jetting Device and Slurry Transport System for Production Systems. Presented at the SPE Annual Technical Conference and Exhibition, New Orleans, 30 September–2 October. SPE-166118-MS. <https://doi.org/10.2118/166118-MS>.
- Richardson, J. F. and Zaki, W. M. 1954. Sedimentation and Fluidisation: Part I. *Trans. Inst. Chem. Eng.* **32**: 35–53.
- Svarovsky, L. 1984. *Hydrocyclones*. Lancaster: Technomic Publishing Co. Inc.
- Witbeck, W. O. and Woods, D. R. 1984. Pressure Drop and Separation Efficiency in a Flooded Hydrocyclone. *Can. J. Chem. Eng.* **62** (1): 91–98. <https://doi.org/10.1002/cjce.5450620114>.

SI Metric Conversion Factors

bar × 1.0	E+02 = kPa
°F (°F–32)/1.8	E–01 = °C
in. × 2.54*	E+00 = cm
L × 1.0	E–03 = m ³
ppmw × 1.0*	E–03 = g/L
psi × 6.894 757	E+00 = kPa

*Conversion factor is exact.

C. Hank Rawlins (P.E.) is the technical director for eProcess Technologies in Houston. He has 25 years of experience in research and process engineering in the upstream oil and gas industry. Rawlins is responsible for development programs in facilities sand management, produced-water treatment, and compact separations systems. He has authored or coauthored 55 publications and is an active member of SPE, where he served as past chair of the Separations Technology Technical Section and is a Distinguished Lecturer for the 2018–2019 season. Rawlins holds a PhD degree in metallurgical engineering from Missouri S&T University.